Determination of element-deuterium bond lengths in Zintl phase hydrides by ^{2}H-NMR

Robin Guehne,[†,‡] Henry Auer,[*,¶] Holger Kohlmann,[¶] Jürgen Haase,[†] and Marko Bertmer[*,†]

†*Felix Bloch Institute, Leipzig University, Linnéstrasse 5, 04103 Leipzig, Germany*

‡*MacDiarmid Institute, School of Chemical and Physical Sciences, Victoria University of Wellington, PO Box 600, Wellington 6140, New Zealand*

¶*Department of Inorganic Chemistry, Leipzig University, Johannisallee 29, 04103 Leipzig, Germany*

E-mail: henry.auer@uni-leipzig.de; bertmer@physik.uni-leipzig.de

Supplementary information to the publication in
Phys. Chem. Chem. Phys. **2019**,

Contents

Dependency of C_Q regarding the dihedral Si-chain to D angle

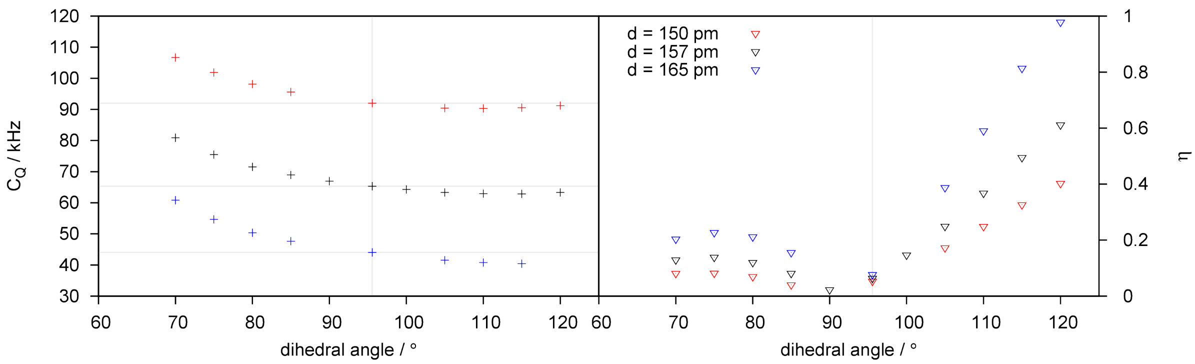

Figure S1: Changes of C_Q and η regarding to the dihedral angle of the plane of the Si zig-zag chain towards deuterium. The $BaSiD_2$-structure was used as a model system. Results are shown for the DFT-optimised bond length d(Si-D) = 157 pm and two additional values. The DFT-optimised structure exhibits a bond angle of 95.6° which is indicated by the grey lines.

Evaluation of Si-D bond lengths from experimental C_Q values

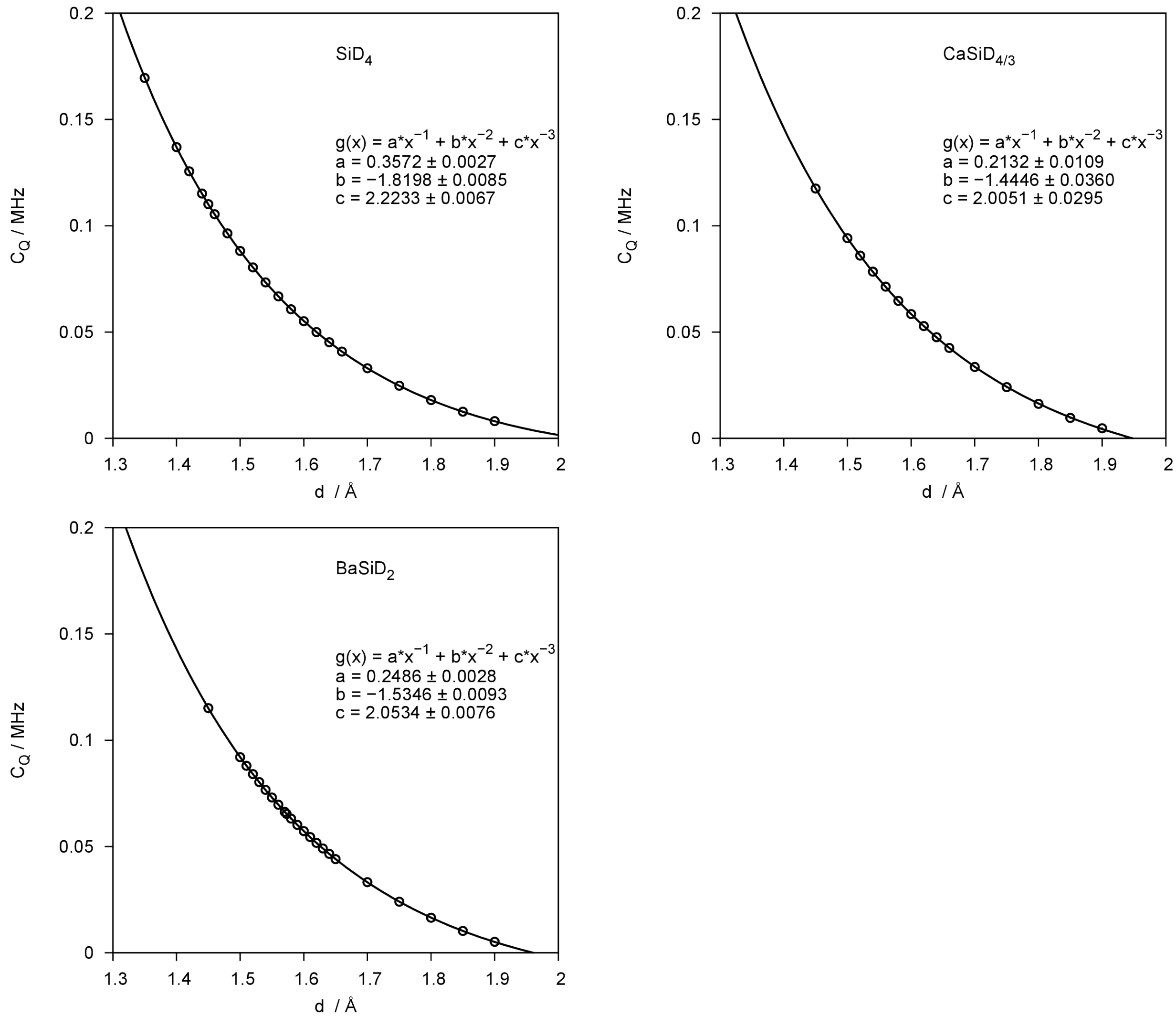

Figure S2: Empirical fits to DFT-derived C_Q-distance curves for the silicon systems.

Table S1: Si-D-distances calculated from experimental C_Q values using the C_Q-distance dependencies as given in Fig. S2.

compound	$C_{Q,exp}$ / kHz		d_{calc}(Si-D) / Å		d_{exp}(Si-D)
		SiD_4-model	$CaSiD_{4/3}$-model	$BaSiD_2$-model	
$CaSiD_{4/3-x}$	69(1)	1.552(3)	1.566(3)	1.562(3)	
$SrSiD_{5/3-x}$	63(1)	1.572(4)	1.584(3)	1.581(4)	
	78(3)	1.526(8)	1.540(8)	1.536(8)	
$BaSiD_{2-x}$	58(2)	1.589(7)	1.601(7)	1.597(7)	
SiD_4	95 [1]	1.482	1.497	1.493	1.473-1.492[a]
CH_3SiD_3	90(2) [4]	1.494(5)	1.509(5)	1.505(5)	1.473-1.492[a]
$C_6D_5SiD_3$	91(2) [5]	1.492(5)	1.507(5)	1.502(4)	1.473-1.492[a]
β-$KSiD_3$	72.0(5) [6]	1.543(2)	1.557(2)	1.553(2)	1.537(8)-1.545(6) [7]

[a]Typical bond lengths. Determined for disilane (Si_2H_6). [2,3]

Evaluation of Ge-D bond lengths from experimental C_Q values

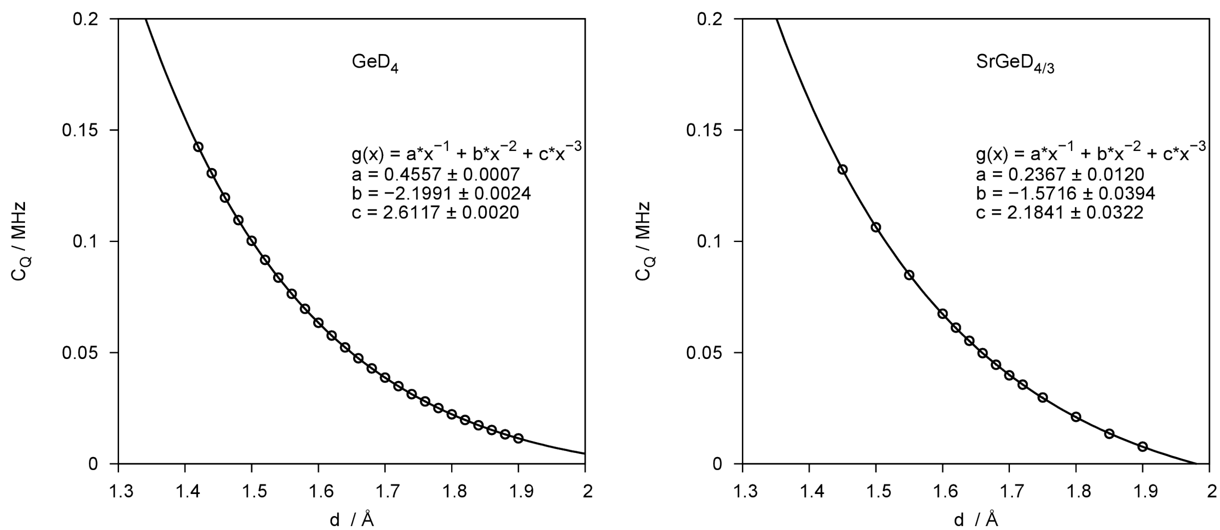

Figure S3: Empirical fits to DFT-derived C_Q-distance curves for the germanium systems.

Table S2: Ge-D-distances calculated from experimental C_Q values using the C_Q-distance dependencies as given in Fig. S3.

compound	$C_{Q,exp}$ / kHz	d_{calc}(Ge-D) / Å		d_{exp}(Ge-D)
		GeD_4-model	$SrGeD_{4/3}$-model	
$SrGeD_{4/3-x}$	52(2)	1.642(8)	1.652(8)	
$BaGeD_{5/3-x}$	51(2)	1.646(8)	1.659(8)	
	61(2)	1.609(7)	1.620(7)	
GeD_4	82(5) [8]	1.545(14)	1.558(13)	1.517 [9]
CH_3GeD_3	82(2) [10]	1.545(7)	1.558(6)	1.517-1.541 [a]

[a] Typical bond lengths. Determined from germane (GeD_4) [9] and digermane (Ge_2H_6). [11]

Sn-D: C_Q-distance dependency according to SnD_4 model

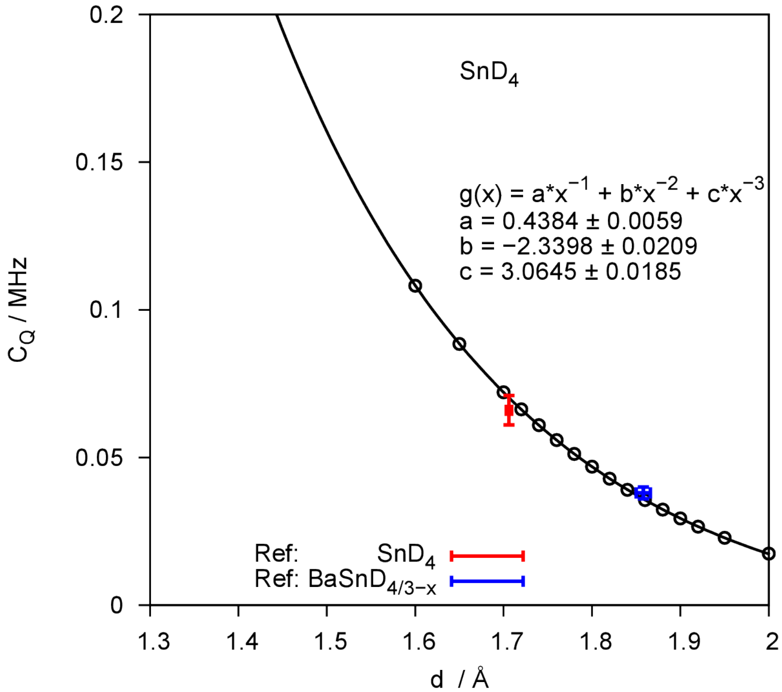

Figure S4: Empirical fit to the DFT-derived C_Q-distance curve of SnD_4. The experimental reference data are: SnD_4: d(Sn-D) = 1.706(3) Å (at 5 K),[9] C_Q = 66(5) kHz.[12]
$BaSnD_{4/3-x}$: d(Sn-D) = 1.858(8) Å,[13] C_Q = 38(2) kHz (this work).
A evaluation of the Sn-D bond length from experimental C_Q-values according to the empirically fitted curve gives:
SnD_4: d(Sn-D) = 1.721(18) Å.
$BaSnD_{4/3-x}$: d(Sn-D) = 1.846(12) Å.

^{2}H MAS spectra at slow spinning showing spinning side-band pattern

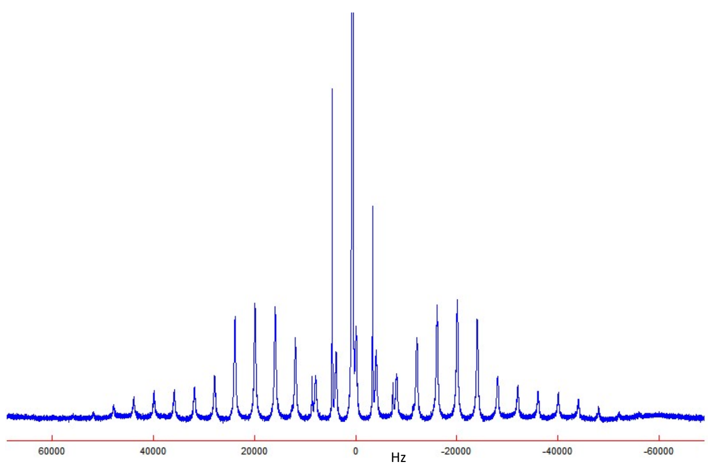

Figure S5: ^{2}H MAS spectrum of $BaSiD_{2-x}$ recorded with a spinning frequency of 4 kHz. The central line is vertically cut for better visibilty of sideband intensities..

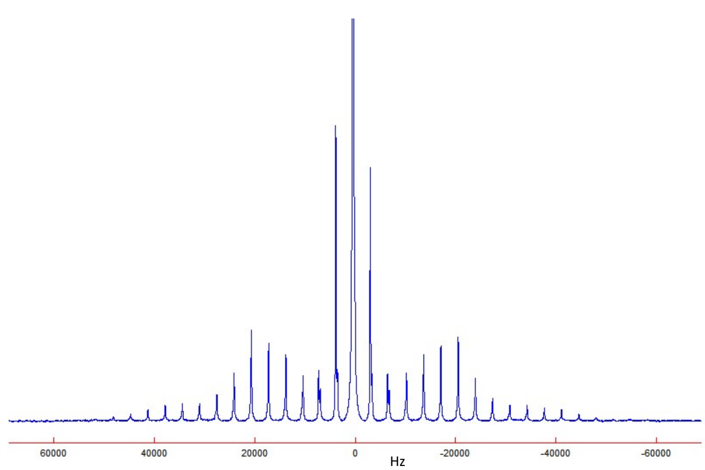

Figure S6: ^{2}H MAS spectrum of $SrSiD_{5/3-x}$ recorded with a spinning frequency of 3.4 kHz. The central line is vertically cut for better visibilty of sideband intensities..

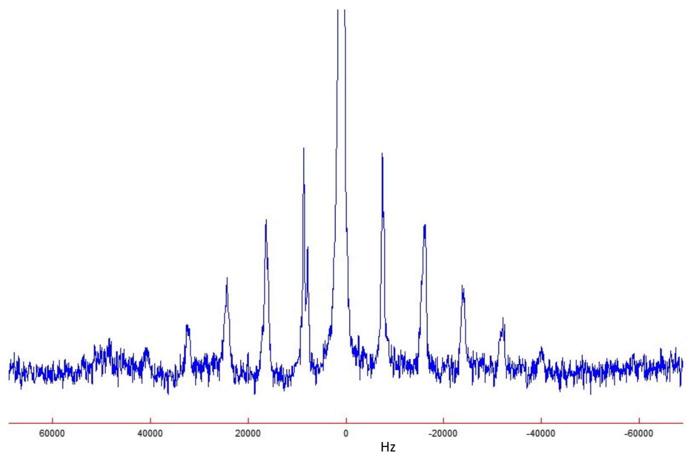

Figure S7: ^{2}H MAS spectrum of $CaSiD_{4/3-x}$ recorded with a spinning frequency of 8 kHz. The central line is vertically cut for better visibilty of sideband intensities..

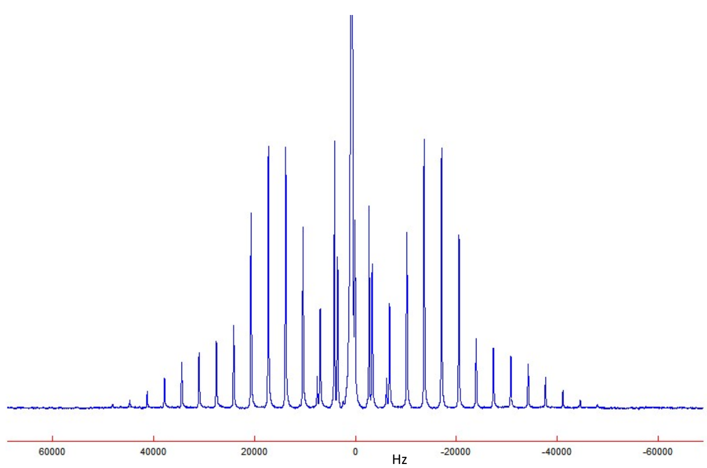

Figure S8: ^{2}H MAS spectrum of $BaGeD_{5/3-x}$ recorded with a spinning frequency of 3.4 kHz. The central line is vertically cut for better visibilty of sideband intensities..

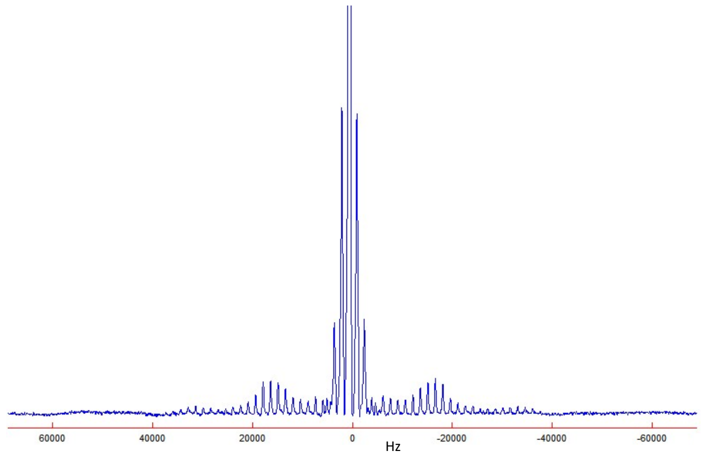

Figure S9: ^{2}H MAS spectrum of $SrGeD_{4/3-x}$ recorded with a spinning frequency of 1.5 kHz. The central line is vertically cut for better visibilty of sideband intensities..

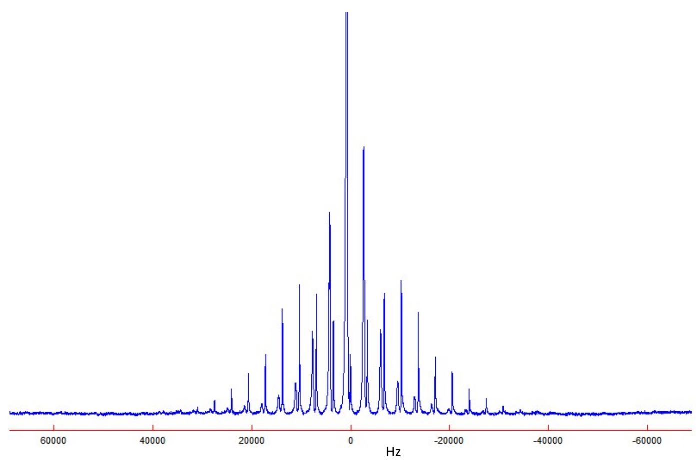

Figure S10: ^{2}H MAS spectrum of $BaSnD_{4/3-x}$ recorded with a spinning frequency of 3.4 kHz. The central line is vertically cut for better visibilty of sideband intensities..

References

(1) Lähteenmäki, U.; Niemelä, L.; Pyykkö, P. Deuteron magnetic resonance in solid and liquid SiD_4 above 36 K. *Phys. Lett. A* **1967**, *25*, 460–461, DOI: 10.1016/0375-9601(67)90080-1.

(2) Brockway, L. O.; Beach, J. Y. The Electron Diffraction Investigation of the Molecular Structures of (1) Phosphorus Oxytrichloride, Oxydichlorofluoride, Oxychlorodifluoride, Oxytrifluoride, Fluorodichloride, Pentafluoride, and Trifluorodichloride, and of (2) Disilane, Trichlorosilane, and Hexachlorodisilane. *J. Am. Chem. Soc.* **1938**, *60*, 1836–1846, DOI: 10.1021/ja01275a036.

(3) Beagley, B.; Conrad, A.; Freeman, J.; Monaghan, J.; Norton, B.; Holywell, G. Electron diffraction studies of the hydrides Si_2H_6 and P_2H_4. *J. Mol. Struct.* **1972**, *11*, 371–380, DOI: 10.1016/0022-2860(72)85004-x.

(4) Ader, R.; Loewenstein, A. N.M.R. study of methylsilane-d3 dissolved in a nematic liquid crystal. *Mol. Phys.* **1974**, *27*, 1113–1116, DOI: 10.1080/00268977400100991.

(5) Fung, B.-M.; Wei, I. Y. Proton and deuteron magnetic resonance of phenylsilane-d3, phenylphosphine-d2, and benzenethiol-d in liquid crystal solutions. *J. Am. Chem. Soc.* **1970**, *92*, 1497–1501, DOI: 10.1021/ja00709a009.

(6) Nedumkandathil, R.; Jaworski, A.; Fischer, A.; Österberg, C.; Lin, Y.-C.; Karlsson, M.; Grins, J.; Pell, A. J.; Edén, M.; Häussermann, U. Investigation of the Order-Disorder Rotator Phase Transition in $KSiH_3$ and $RbSiH_3$. *J. Phys. Chem. C* **2017**, *121*, 5241–5252, DOI: 10.1021/acs.jpcc.6b12902.

(7) Tang, W. S.; Chotard, J.-N.; Raybaud, P.; Janot, R. Enthalpy-Entropy Compensation Effect in Hydrogen Storage Materials: The Striking Example of Alkali Silanides $M\mathrm{SiH}_3$ (M = K, Rb, Cs). *J. Phys. Chem. C* **2014**, *118*, 3409–3419, DOI: 10.1021/jp411314w.

(8) Hovi, V.; Lähteenmäki, U.; Tuulensuu, R. Deuteron spin-lattice relaxation and phase transitions in GeD_4. *Phys. Lett. A* **1969**, *29*, 520–521, DOI: 10.1016/0375-9601(69)90411-3.

(9) Maley, I. J.; Brown, D. H.; Ibberson, R. M.; Pulham, C. R. Solid-state structures of the covalent hydrides germane and stannane. *Acta Crystallogr., Sect. B* **2008**, *64*, 312–317, DOI: 10.1107/S0108768108010379.

(10) Ader, R.; Loewenstein, A. Proton and deuterium magnetic resonance studies of methylsilane and methylgermane dissolved in a nematic liquid crystal. *J. Am. Chem. Soc.* **1974**, *96*, 5336–5340, DOI: 10.1021/ja00824a006.

(11) Beagley, B.; Monaghan, J. J. Electron diffraction study of digermane. *Trans. Faraday Soc.* **1970**, *66*, 2745, DOI: 10.1039/tf9706602745.

(12) Niemela, L.; Mäkelä, J. Deuteron spin-lattice relaxation in solid SnD_4. *Phys. Lett. A* **1973**, *43*, 343–344, DOI: 10.1016/0375-9601(73)90335-6.

(13) Auer, H.; Guehne, R.; Bertmer, M.; Weber, S.; Wenderoth, P.; Hansen, T. C.; Haase, J.; Kohlmann, H. Hydrides of Alkaline Earth-Tetrel (*AeTt*) Zintl Phases: Covalent *Tt*-H Bonds from Silicon to Tin. *Inorg. Chem.* **2017**, *56*, 1061–1071, DOI: 10.1021/acs.inorgchem.6b01944, PMID: 28098994.